Proceedings of the Indian National Science Academy (2023) 89:811–824
https://doi.org/10.1007/s43538-023-00195-5

RESEARCH PAPER

Fuzzy controller-based predictive speed control of a permanent magnet synchronous motor

Jinli Wang[1] · Dahai Yu[1]

Received: 14 May 2023 / Accepted: 26 July 2023 / Published online: 21 August 2023

Abstract

In order to control permanent magnet synchronous motor systems with different and nonlinear disturbances, this paper offers an enhanced current control technique for PMSM systems using fuzzy model predictive control. Because traditional MPC calculations should be performed live, load and speed changes are guaranteed by applying input modifications concurrently with motor adjustments. In order to enhance system performance, a fuzzy error controller and a predictive model control system are employed in this work. Additionally, a sliding mode observer using the sigmoid operation to control speed without a PMLSM sensor is presented in the current study. The traditional sliding approach includes a phase delay and buzz observer. Therefore, this study uses a sliding mode observer with a sigmoid function for detecting back-EMF in PMLSM instead of a conventional sliding mode observer that uses sign or saturation functions that need a low-pass filter to detect back-EMF to estimate rotor speed and position. To lessen the undesirable gap, a sigmoid function rather than a discrete sign function is employed in this study. With no low-pass filter, the switching signal can be used to detect the back-EMF as the gap closes.

Keywords Fuzzy model predictive control · Back-EMF · Permanent Magnet Linear Synchronous Motor

Introduction

Modern permanent magnet synchronous motors have drawn interest in a variety of applications, including transportation, domestic, and industrial (Xu et al. 2016). There is an increasing demand for efficient energy, high-performance, and dependable electric drives due to the global trend towards energy conservation (Ye and Yao 2020). Due to their high output power at any volume, good efficiency, and superior dynamic performance, PMSMs make excellent choices (Kakosimos and Abu-Rub 2017). In recent years, using PMSMs has increased due to their advantages for DC and AC applications compared to industrial motors (Ullah et al. 2022). Some of these advantages include high efficiency, low ripple, low maintenance cost, and high reliability (Mahmoudi et al. 2017). These advantages have made PMSMs an ideal candidate for tensile applications, robotic applications, and hybrid electric vehicles that require high efficiency and accurate response (Alexandrou et al. 2016). Some conventional controllers used to control motor speed in the industry are PI and PID controllers, which are widely used due to their simplicity. They convert motor speed changes with respect to the reference speed to the estimated torque of the motor (Li et al. 2021). But these controllers do not represent a proper response in a wide range of speeds due to issues like sensitivity to motor parameters under various conditions, step changes of speed and load torque (Saraei et al. 2022). Other controllers used to control motor speed include a sliding mode controller and an adaptive back-stepping controller (Raj et al. 2020). But using these controllers is difficult since they depend on motor parameters (Ab Ghani et al. 2022). Another controller used to control internal permanent magnet drive speed is the smart controller, like the fuzzy logic controller and neural network controller (Du et al. 2020). Among smart controllers, the fuzzy logic controller is one of the simplest ones for controlling the drive speed of the PMSMs with high performance (Sahebjam et al. 2021). Since these controllers are based on linguistic rules founded on human linguistics, they outperform conventional controllers in terms of being insensitive to parameter changes, load torque changes, proper time response, short settling time, and stability (Khezri and Zeinali 2021).

✉ Dahai Yu
ydh1357@sina.com

[1] College of Electrical Information, Changchun Guanghua University, Changchun 130033, Jilin, China

A predictive speed controller (PSC) built on managing the forecast of a limited group of electric drives has been introduced in Kakouche et al. (2023). Many prediction steps can be removed by properly weighting speed errors and current mistakes in the suggested PSC cost function. A suitable predictive current controller (PCC) for monitoring the high efficiency of a PMSM with constant switching frequency has been given in Alqudah et al. (2013). Direct predictive control (DPC) and permanent control approaches are properly combined to form the foundation of the suggested controller. A modulated model predictive control system (MMPC) for PMSM based on a Z-source inverter has been reported in another study (Zhao et al. 2023). A 2DoF-PI controller has been employed in Trik et al. (2022) and Khezri et al. 2023) to regulate the PMSM's speed. An enhanced just-in-time learning technique using two new search engines has been given in the first stage to identify the speed control system model quickly. The future speed reference, which is inaccessible between two terminal communication periods, has been thought of in the second stage using a general formula. A fractional order general prediction control (FOGPC) has been included in the third phase to enhance the servo-drive system's control capabilities.

In this research, a pulse width modulation (PWM) speed controller was used for the motor rather than the conventional six-switch three-phase inverter. The switching frequency may be regulated with this approach, unlike the traditional DTC, which makes it impossible to reduce torque and current fluctuations at low speeds. The outcomes of the simulation shows how well this instruction performs in pair and flux behaviour. Thus, this study tries to present a smart fuzzy controller for controlling the speed and torque of PMSMs.

The contribution of the authors in this research is summarized as follows.

- A fuzzy error controller has been used to improve the system's performance along with the predictive model control system.
- Introduce a sigmoid-function-based sliding mode controller for sensor-free speed regulation of a Permanent Magnet Linear Synchronous Motor (PMLSM).

The rest of this paper is organized as follows. The section reviews the literature. "The proposed model" section presents the system model for PMSM and its mathematical model. "Evaluation and simulation" section presents the proposed model. Section 4 gives the simulation results of the proposed model. Finally, future suggestions are given in "Conclusion" section.

System model

Synchronous motors with permanent magnets

PMSMs are ideal candidates for many industrial processes. Figure 1 shows a PMSM. PMSM is a conventional synchronous motor that employs a permanent magnet instead of exciting the rotor, brushes, and slip rings (Samiei et al. 2023; Sun et al. 2022). The PMSM stator is like the inductance motor stator, but the windings are located on the stator and the heat resulting from the armature is transferred to the surrounding air through the stator body. Also, additional protection can be considered for the overloading of PMSM because the temperature of the heat-generating section can be sampled and controlled directly (Trik et al. 2021).

These motors are manufactured from low to high power and speed of up to 6000 rpm (Cao et al. 2023; Ning et al. 2023). For instance, a motor with a rated power of 1 MW has been constructed and used in energy generation processes. Also, this motor is used as a propulsion force of a ship (Khezri et al. 2022; Duan et al. 2022).

Model predictive control for PMSMs

The specification of the cost function in relation to control objectives is the core technology of MPC. The stator torque and flux are the main issues with the PMSM disc drive. As

Fig. 1 PMSM (Ab Ghani et al. 2022)

a result, the torque and flux at the conclusion of the control cycle are as close to the reference values as possible (Cao et al. 2022). The cost function is defined as follows in this study:

$$\begin{aligned} &min.\ G = \left|T_e^* - T_e^{k+1}\right| + k_1\left|\left|\psi_s^*\right| - \psi_s^{k+1}\right| \\ &u_s^k \in \{V0, V1, \dots V7, V8\} \end{aligned} \tag{1}$$

where $T^{K+1}e$ and $\Psi^{k+1}{}_s$ are the anticipated torque and flux values, T_e^* and ψ_s^* are the reference torque and flux values, and k_1 is the weight factor. The weight factor k_1 is included to reduce this disparity since the electromagnetic torque and stator flux have distinct physical characteristics. In this study, the stator torque and current, T_n/ψ_n, are used to calculate k1.

$$\begin{cases} u_d = R_s i_d + L_d \frac{d_{id}}{dt} - \omega L_d i_q \\ u_q = R_s i_q + L_q \frac{d_{iq}}{dt} - \omega_e L_d i_q + \omega_e \psi_f \end{cases} \tag{2}$$

According to the above equation, stator current in the d–q frame can be described as state space equations in the following:

$$\begin{cases} \frac{d_{id}}{dt} = \frac{-R_s i_d + \omega_e L_d i_q + u_d}{L_d} \\ \frac{d_{iq}}{dt} = \frac{-\omega L_d i_d - R_s i_q + u_q - \omega \psi_f}{L_q} \end{cases} \tag{3}$$

It is possible to estimate the stator current in the d–q frame at (k + 1).

$$\begin{cases} i_d^{k+1} = i_d^k + \frac{1}{L_d}(R_s i_d^k + \omega^k L_q i_q^k + u_d^k)T_s \\ i_q^{k+1} = i_q^k + \frac{1}{L_q}(\omega^k L_d i_d^k - R_s i_q^k + u_q^k - \omega^k \psi_f)T_s \end{cases} \tag{4}$$

The torque and flux at an instant (k + 1) can be estimated using the present stator current.

Figure 2 displays the MPC block diagram. The reference and predicted toque and flux values make up the system inputs.

$$\begin{cases} \psi_d = L_d i_d + \psi_f \\ \psi_q = L_q i_q \end{cases} \tag{5}$$

$$T_e = \frac{3}{2} p(\psi_d i_q - \psi_q i_d) \tag{6}$$

Equation (7) provides the const function that is employed in the predictive controller of the model to control the predicted speed of the permanent magnet synchronous motor.

$$\begin{aligned} &J = \sum_{i=N_1}^{N_2} \left[y(k+i) - y^*(k+1)\right]^2 + \lambda = \sum_{i=1}^{N_u} \Delta u^2(k+i-1) \\ &\Delta u(k+i-1) = 01 \le N_u < i \le N_2 \end{aligned} \tag{7}$$

where N_u predictive speed control, N_1 minimum model prediction and N_2 maximum model prediction, i predictive order, y^* reference order, λ weight factor, k time step and Δ differentiation operator. The control input signal u is subject to the following constraints:

$$u_{min} \le u(k+i) \le= u_{max}, \quad where \quad i = 1, 2, 3, \dots N_u$$

It is possible to forecast the future states and controlled variables in the permanent magnet synchronous motor using these two justifications and the predictive speed control dynamic system model, and to minimize the cost function accordingly.

PMSM as a mathematical model

The equation is usually written in the following extended form:

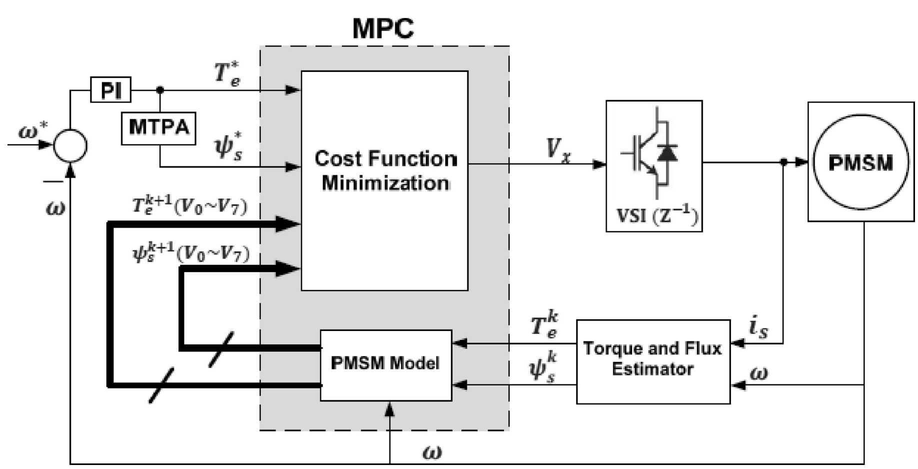

Fig. 2 Block diagram of the MPC system (Trik et al. 2023)

$$V_{ds} = R_s I_{ds} + L_d \frac{dids}{dt} - \omega_r L_q i_q$$
$$V_{qs} = R_s I_{qs} + L_q \frac{diqs}{qt} + \left(L_d i_{ds} + \gamma_m\right) \quad (8)$$
$$V_{0s} = R_s I_{0s} + L_0 \frac{di0s}{dt}$$

The rotor's angular velocity is constant and equal to that of the synchronously rotating reference frame in a balanced, stable state. The basic state versions of the aforementioned equations are converted in this state, while changes to all flux linkages are disregarded.

$$V_{ds} = R_s I_{ds} - \omega_r L_q i_q$$
$$V_{qs} = R_s I_{qs} + \omega_r \left(L_d i_{ds} + \gamma_m\right) \quad (9)$$
$$V_{0s} = R_s I_{0s} = 0$$

The electromagnetic torque using stator variables in the reference frame of the rotor can be described as follows:

$$T_e = \left(\frac{3}{2}\right)\left(\frac{P}{2}\right)\left(\gamma_{ds} I_{qs} - \gamma_{qs} I_{ds}\right) \quad (10)$$

Substituting in the above torque equation, we have:

$$T_e = \left(\frac{3}{2}\right)\left(\frac{P}{2}\right)[\gamma_m I_{qs} + (L_d - L_q) I_{qs} I_{ds}] \quad (11)$$

The torque equation can be described as follows:

$$T_e = T_m + j\frac{d}{dt}\omega_r + B\omega_r \quad (12)$$

Fuzzy logic controller

Fuzzy logic controller systems can be used as open-loop or closed-loop controllers. When used as an open-loop controller, the fuzzy system usually determines some control parameters and then controls the system according to these parameters. Many applications of fuzzy systems in electronics belong to this category. When fuzzy systems are used as closed-loop controllers, in this case, they measure the process outputs and perform control operations simultaneously. Applications of fuzzy systems in industrial processes belong to this category. Figure 3 shows the basic configuration of a fuzzy logic control (Raj et al. 2023; Chen et al. 2023; Morteza et al. 2023). A clear input signal undergoes fuzzyification, which creates signals that are distinguishable by their level of membership in fuzzy sets. Fuzzy logic uses linguistic variables instead of numerical variables. In a control system, the error between reference and output can be labeled as very small (VS), small (S), medium (M), large (L), or very large (VL). The process of converting a numerical variable (a real number) into a linguistic variable (a fuzzy number) is called fuzzification.

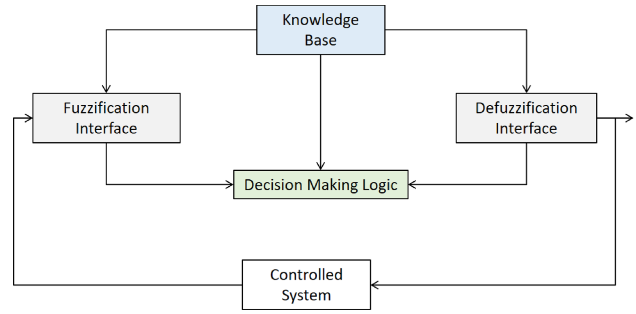

Fig. 3 Block diagram of fuzzy logic control function

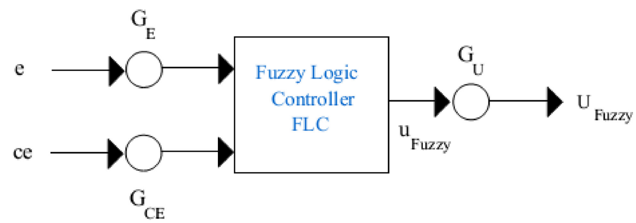

Fig. 4 The scaling factors for FLC

FLC has an input error e(k) and the velocity error change ce(k), and an output u(k) that shows the changes in the fourth order reference current I_q^* (k).

e(k) and ce(k) are calculated for all sampling times:

$$\text{e(k)} = \omega_r^*(k) - \omega_r(k) \quad (13)$$

$$\text{ce(k)} = e(k) - e(k-1) \quad (14)$$

where ω_r^* (k) denotes the reference speed and ω_r (k) denotes the actual speed.

As shown in Fig. 4, the constant gain blocks are used as the GE, GCE, and GU scaling factors to obtain the normalised inputs and outputs for the FLC.

$$e(k) = g_e e(k) \quad (15)$$

$$ce(k) = g_{ce} ce(k) \quad (16)$$

$$u(k) = g_u u(k) \quad (17)$$

Fuzzification, inference, and defuzzification are the three steps in FLC. Using the triangle membership functions, certain variables e(k) and ce(k) are transformed into fuzzy variables of E(k) and CE(k) (Figs. 5, 6).

In the second stage, an inference engine processes the fuzzy variables E and CE while carrying out a series of control laws found in the rule bases (7 × 7). Knowing how PMSMs behave helps create control laws (Zhang et al. 2023). The centroid defuzzification algorithm, which

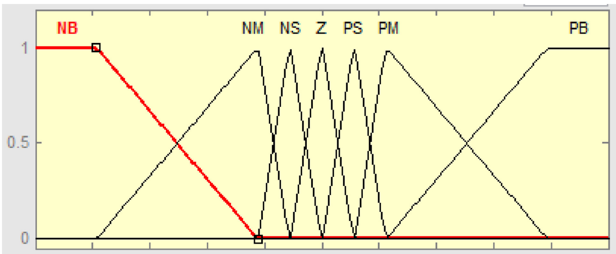

Fig. 5 The membership functions in FLC 1

calculates a specific value as the centre of mass of the membership function, is employed in this study.

The proposed model

The proposed MPC's block diagram is shown in Fig. 7. It can be seen that the speed control section creates the stator's current reference in the q-axis. The stator's reference is now set to zero. The following is a description of the remaining sections.

Levenberger observer

Being sensitive to system parameter uncertainty is one drawback of MPC. An observer is utilised to calculate the stator's and the system parameters' uncertainty in order to overcome this issue (Zhang et al. 2023). Based on (18), (19) and (20) represent a mathematical observer model:

$$\mathrm{x}(\mathrm{k}+1)=ax(k)+bu(k) \tag{18}$$

$$\mathrm{x}(\mathrm{k}+1)=a\dot{x}(k)+bu(k)+g(yk)-\dot{y}(k) \tag{19}$$

$$c\dot{x}(k)=\dot{y}(k), \tag{20}$$

where G is the observer gain, and the variables with a superscript ^ are the estimated state variables. The observer gain is chosen to have a faster dynamic than the system. Asymptotically constant error estimation error requires that the gain be modified as well. The estimation error is computed using the formula below:

$$e(k)=\dot{x}(k)-x(k) \tag{21}$$

Fig. 6 The membership functions in FLC 2

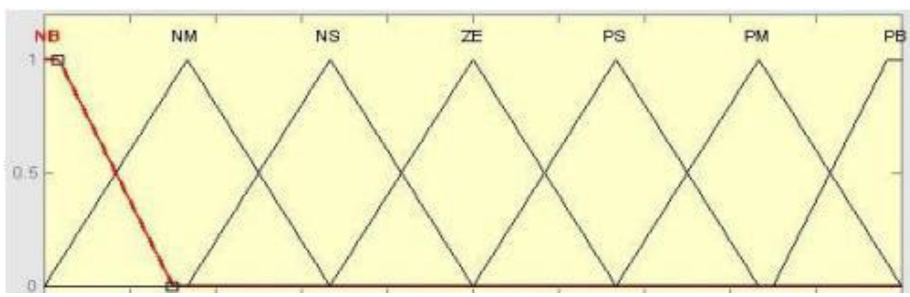

Fig. 7 Block diagram of the proposed MPC

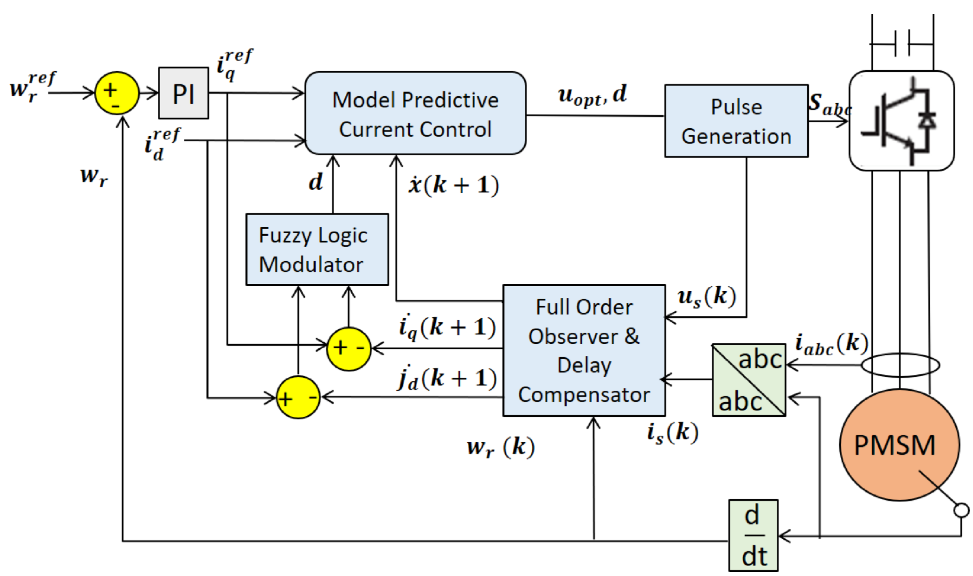

By substituting (18) and (19) in (20), the error dynamicity equation is obtained as follows:

$$e(k+1) = x(k+1) + \dot{x}(k+1) \rightarrow e(k+1) = a_0 e(k) \quad (22)$$

According to (22), the error's dynamic equation would be constant if the observer gain, G, is changed so that the eigenvalues of the matrix A_O are contained within the unit circle. The estimated states are near their genuine values $(x\ (k+1)) \rightarrow x\ (k+1)$ and the zero estimation error $(e\ (k+1) \rightarrow 0)$ (ignoring the initial estimation error, e(0)).

Current control model prediction

Choosing the best switching pattern to minimise a predefined cost function is the goal of predictive control. In this analysis, we use the following formulation for the cost function:

$$j = \left| I_q^{ref} - i_q(k+1) \right| + \left| i_d(k+1) \right| + f(i_d, i_q) \quad (23)$$

where

$$f\left(i_d, i_q\right) = \begin{cases} 0, if I_{max} - \sqrt{I_q^2 + I_d^2 > 0} \\ cst, otherwise \end{cases} \quad (24)$$

To make sure that the stator current stays within the inverter current's current range, $f(i_d, i_q)$ is added to the cost function. A constant value that is greater than the other two cost function criteria is added if the stator current exceeds this range. For each accessible voltage vector, $i_d\ (k+1)$ and $i_q\ (k+1)$ in (18) are estimated in (23). In the following sample step, the switching pattern that minimises the cost function J is chosen and used.

Evaluation and simulation

The MPC algorithm modeled in Simulink

The MPC simulations of a PMSM are shown in Fig. 8. The total operation time is 1s. In 0.5 s, the reference speed goes from 700 to 1200 rpm; in 0.07 s, the load goes from 5 to 8 Nm.

Figure 9 depicts the three-phase currents. Also, the simulations are performed when the motor is controlled using a PI fuzzy predictive controller. The three-phase currents are obtained after transformation in the DQ coordinate, as in Fig. 10, representing I_d and I_q. Compared to the three-phase currents obtained using two fuzzy and conventional PI controllers, the inverter generates the MPNS current for MPC and sinusoidal waves for SVPWM. Figure 11 also represents the motor speed changes vs reference speed changes; as the speed increases from 700 to 1200RPM, a settling time of 0.02s with minimum ripple in steady state and transient state is obtained as in Fig. 12 for the fuzzy control. As can be seen, using the FLC increases the system response speed to speed changes. Also, this method reduces oscillations and ripples of speed and torque in a steady state. Figures 13, 14, 15 and 16 show the system outputs with predictive control based on conventional PI controllers. As can be seen, the settling time of this controller for the motor speed is 0.04s, and a high torque, current and speed ripple is seen in this controller compared to the fuzzy controller, indicating the optimal performance of the predictive control system with fuzzy control. In all diagrams, the horizontal axis is the

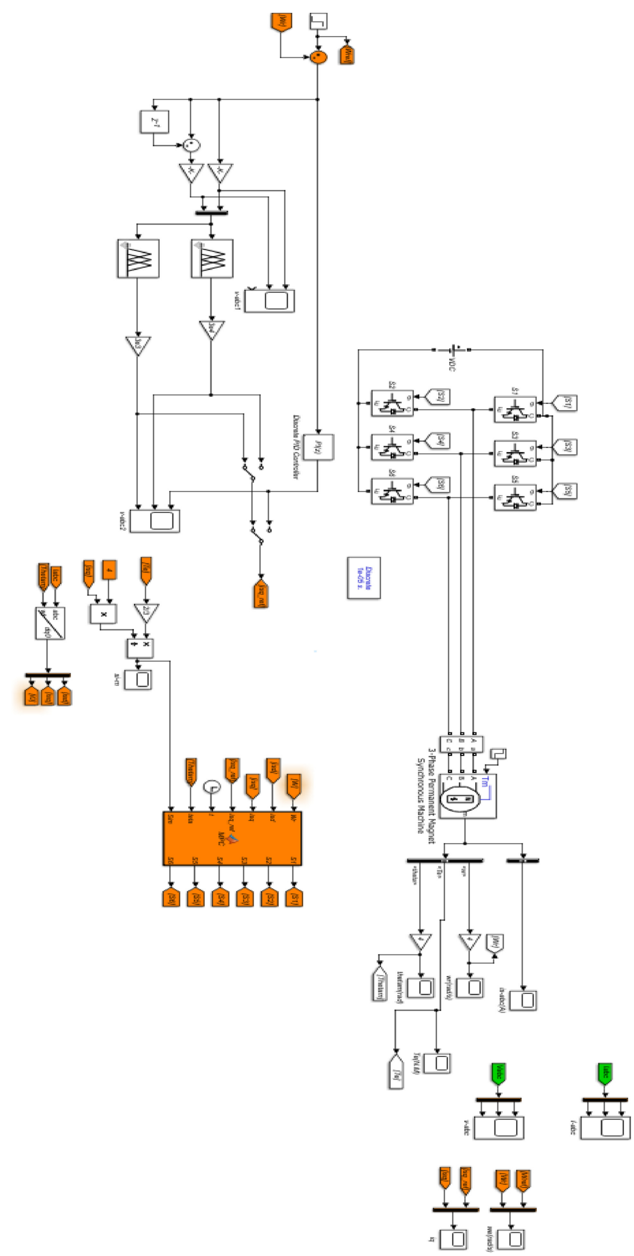

Fig. 8 MPC blocks for PMSM

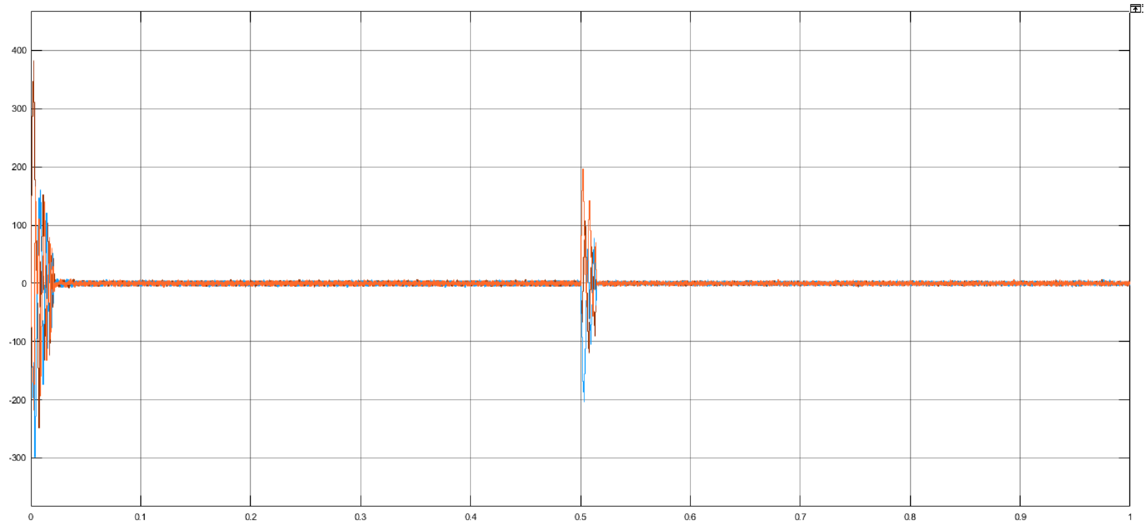

Fig. 9 Fuzzy-controlled three-phase currents for the MPC motor

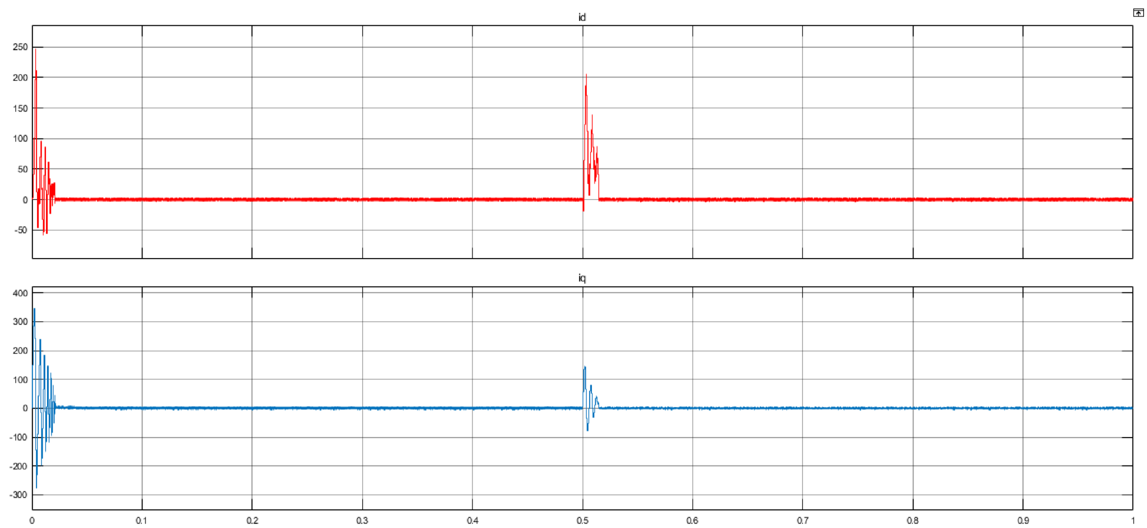

Fig. 10 Motor currents for the fuzzy controller after three-phase to d-q frame conversion. (a) I_d and (b) I_q

simulation time between 0 to 1s and the torque increases or decreases corresponding to the changes in load torque and speed.

Determining rotor speed and position using the proposed method

The sliding mode observer can be used to explain back-EMF, although these signals still contain high-frequency components. As a result, they cannot be utilised directly to determine the position and speed of the rotor. In a traditional sliding mode, the cut-off frequency and angle of the input signal are used to produce a low-pass filter to filter the processes that cause phase delay. The information from the true linear speed should be used to make up for the phase lag caused by the delay; the information from the estimated linear speed is insufficient. In order to avoid using the low-pass filter and phase compensator based on back-EMF, a sliding mode observer is developed for detecting back-EMF in a PMLSM for computing rotor speed and location. It is assumed that $\dot{\omega} = 0$ because changes in the motor's linear speed are less significant than changes in stator current. Therefore, the following description fits the back-EMF of the PMLSM:

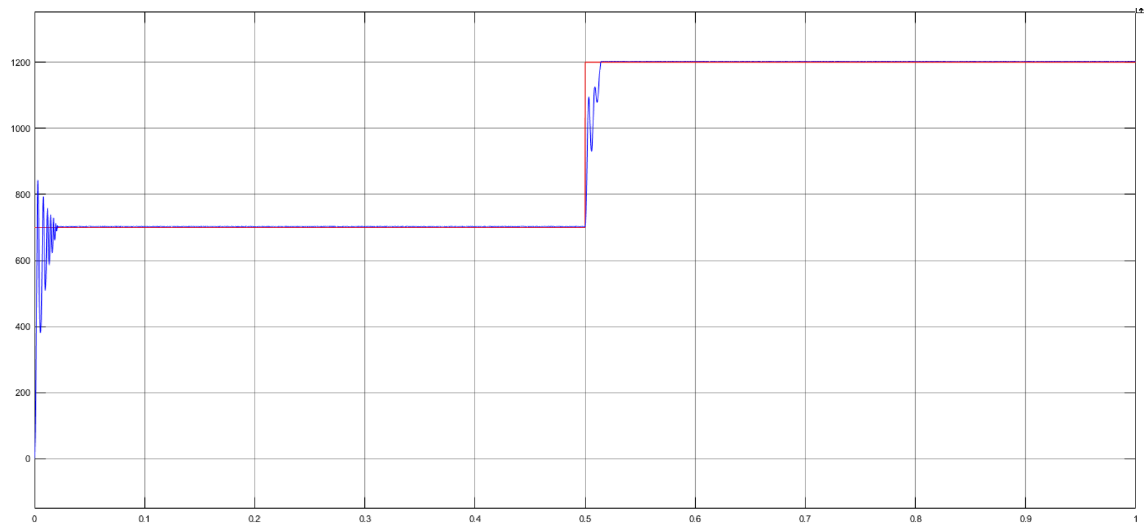

Fig. 11 The motor's output speed and reference speed for the fuzzy controller

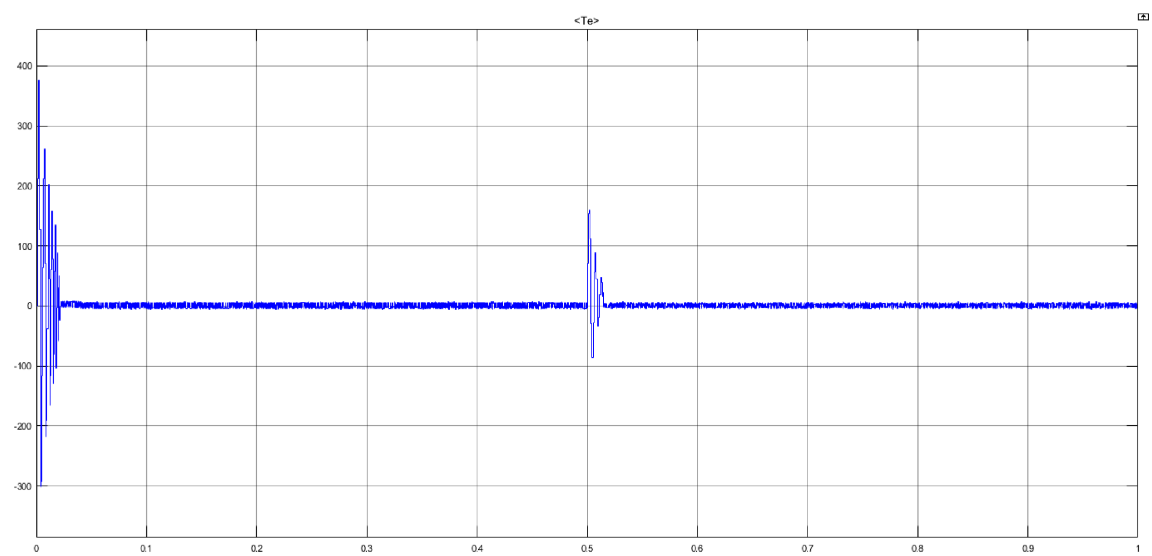

Fig. 12 Motor torque for the fuzzy controller

$$\frac{de_a}{dt} = -\omega e_\beta$$

$$\frac{de_\beta}{dt} - \omega e_a \tag{25}$$

Considering this equation, the following forms the basis for the proposed back-EMF observer:

$$\frac{d\dot{e}_a}{dt} = -\dot{\omega} e_\beta - l(\dot{e}_a - e_a)$$

$$\frac{de_\beta}{dt} = -\omega e_a - \dot{\omega} e_\beta - l(\dot{e}_a - e_a) \tag{26}$$

where l is the observer gain and should be greater than 1, it is selected as 100.

Subtracting (25) from (26), we get the observer's error equation:

$$\frac{d\dot{e}_a}{dt} = -\dot{\omega} e_\beta - \dot{\omega}\dot{e}_\beta - l\dot{e}_\beta$$

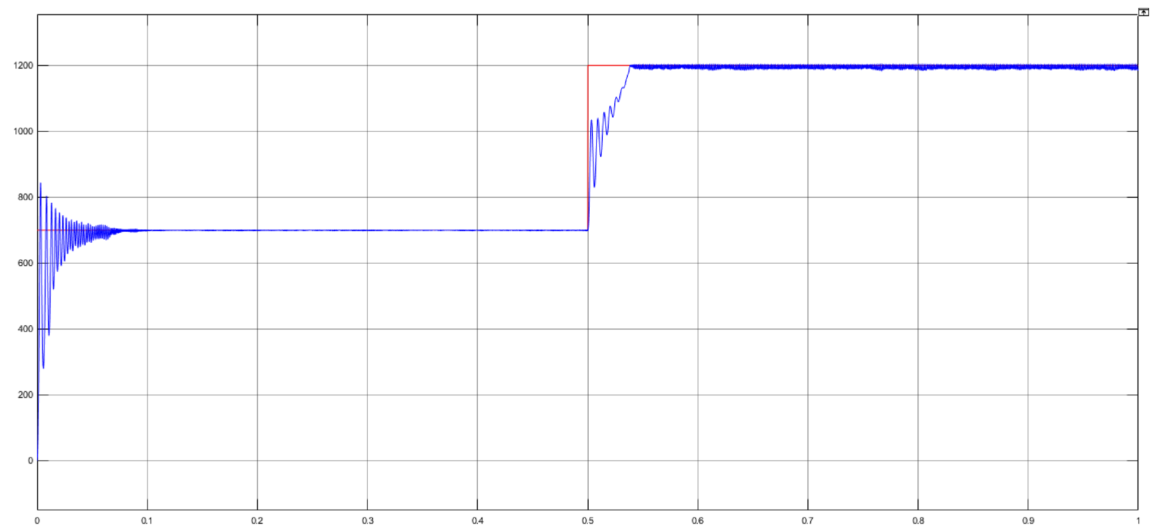

Fig. 13 The motor's output speed and reference speed for the traditional PI controller

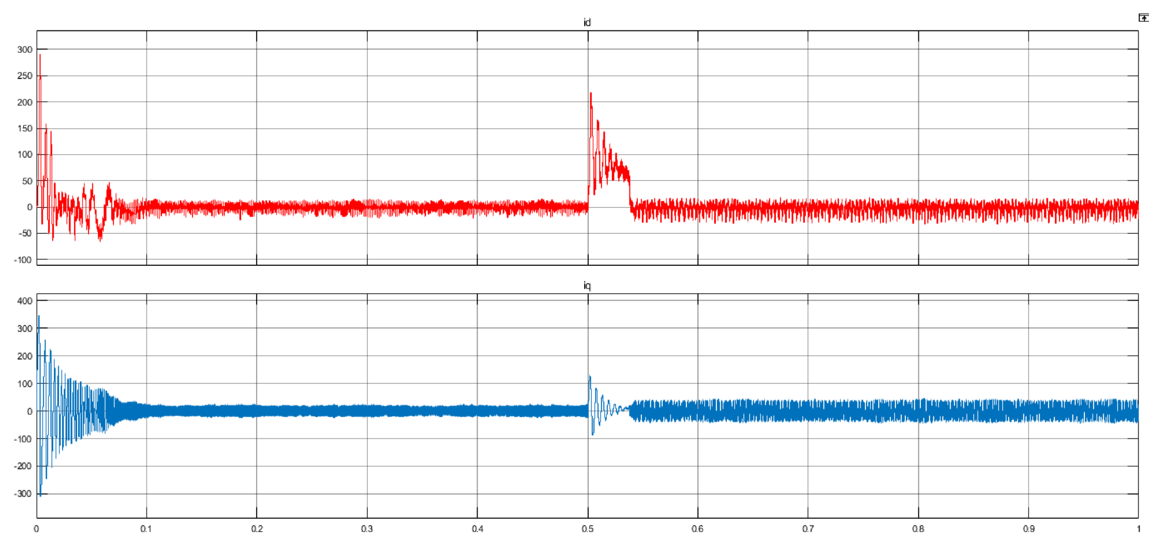

Fig. 14 Fuzzy controller motor currents in the resulting d-q frame from the three-phase input. (a) I_d and (b) I_q

$$\omega = \omega - \omega \frac{d\dot{e}_a}{dt} - \dot{\omega} e_\beta - \dot{\omega} \dot{e}_\beta - l \dot{e}_\beta \tag{27}$$

Since (26) is stable, the Lyapunov operation can be defined as follows:

$$v = \frac{\left(e_a^2 + e_\beta^2 + \omega 2\right)}{2} \tag{28}$$

$$\dot{v} = \dot{e}_a e_a + \dot{e}_\beta e_{a\beta} + \omega \dot{\omega} \tag{29}$$

Differentiating the above equation results in the following: By substituting (27) in (29), we have:

$$v = -l\left(\dot{e}_a^2 + e_\beta^2\right) \le 0 \tag{30}$$

The aforementioned equation demonstrates the back-EMF observer's stability in the absence of a sign. As a result, the location signal may be estimated using the back-EMF collected from the observer and the back-EMF and rotor state equation:

$$\varnothing = arctan\left(\frac{e_a}{\dot{e}_\beta}\right) \tag{31}$$

With the help of an integrator in the observer, speed is achieved.

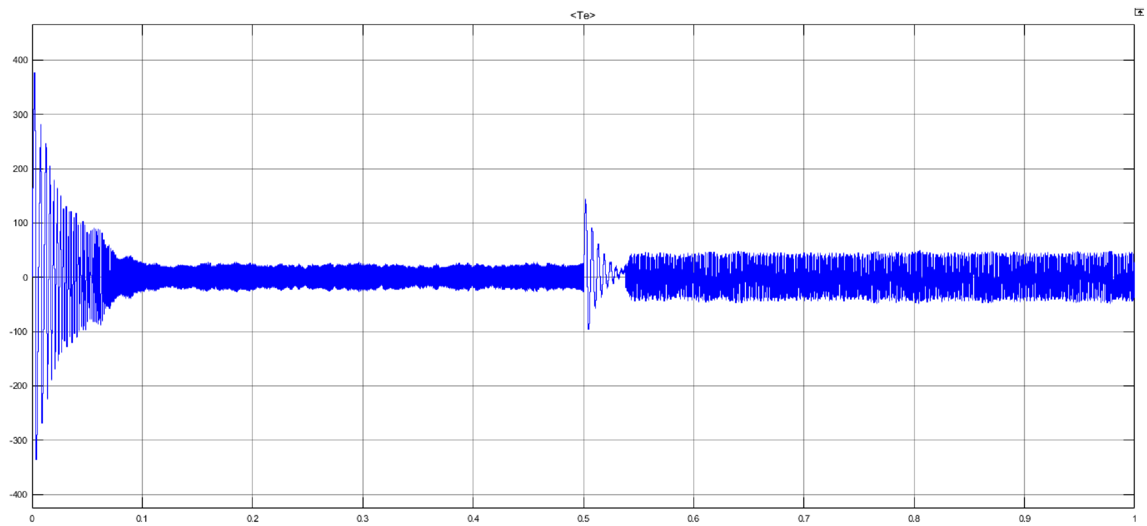

Fig. 15 The torque needed for a traditional PI controller

Fig. 16 Output speed of the motor **a** under fuzzy control, **b** under conventional PI control by changing speed from 800 to 600 pm

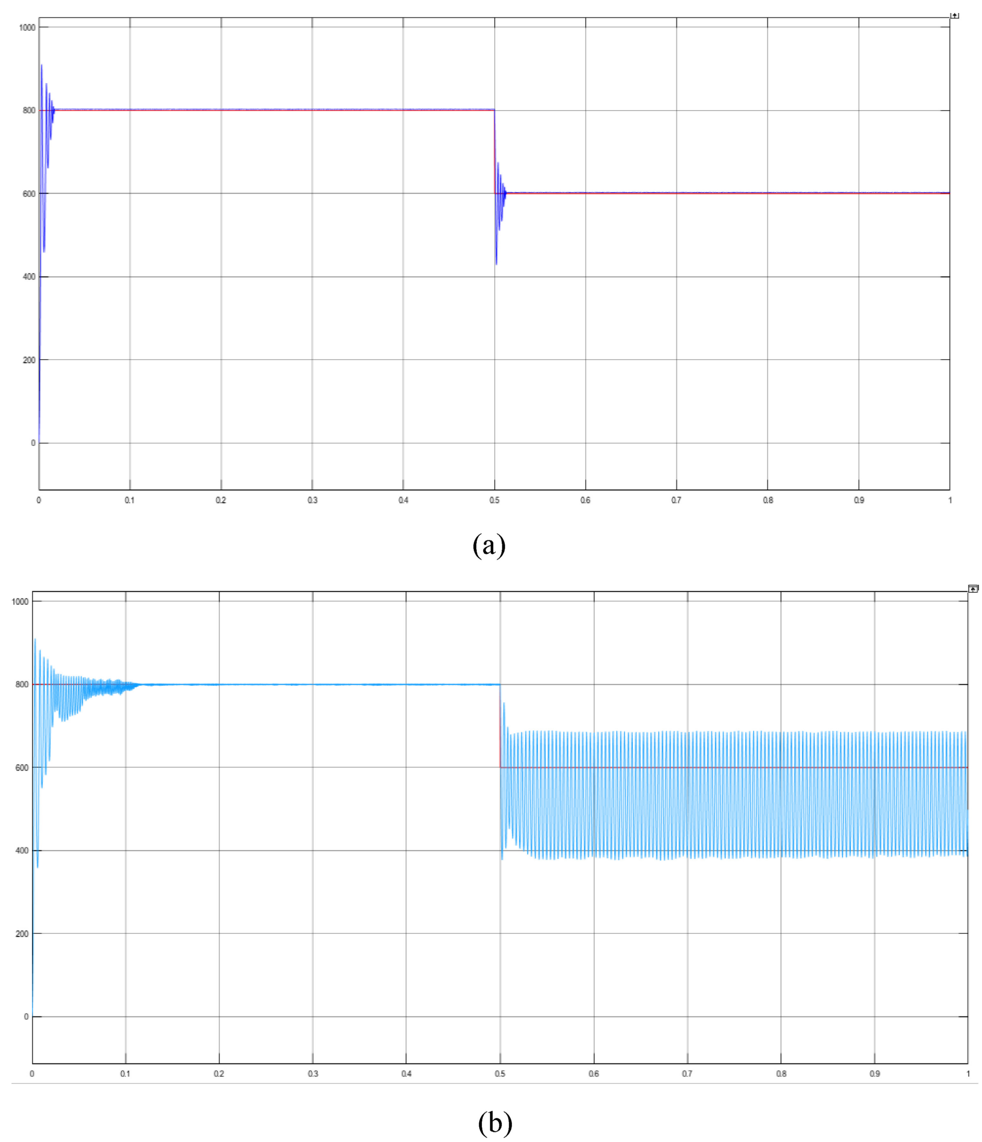

Figures 17 and 18 illustrate the target sliding mode observer block diagram as well as the generic PMLSM sensor design. It is important to note that the motor voltage is utilised as the input to the sliding mode observer rather than the output voltage u_α^* and u_β^* from the current loop. Both u_α and u_β reduce the inverter's dead time. This results in more accurate measurements of motor voltage and computations of motor speed and position.

Figures 19 and 20 show the simulation results of the sliding mode estimator for the conventional PI predictive control system. As can be seen, the estimator system estimates the speed in a steady state with an error of zero based on the three-phase current and voltage of the motor, indicating the proper performance of the estimation. A delay of 0.1s of this estimator is also based on the delays defined to realize the speed estimation system in the simulator.

Additionally, Figs. 17 and 18 show how the speed sliding mode controller and speed loop disturbance compensation technology may greatly enhance the system's anti-disturbance performance. Figures 19 and 20 illustrate how the current loop disturbance technology can reduce adjustment time and speed up the system's dynamic reaction. Additionally, it can speed up and improve the stability of tracking iq reference. Table 1 displays quantitative performance comparison information.

Additionally, the fuzzy logic controller (MPC) for the thrust force error graphs during the transient phase is calculated as calculated in Table 1 in order to statistically examine the control performance for these PI increases. Furthermore, it is well known that the MPC for the thrust reaction likewise reduces as the rising time does.

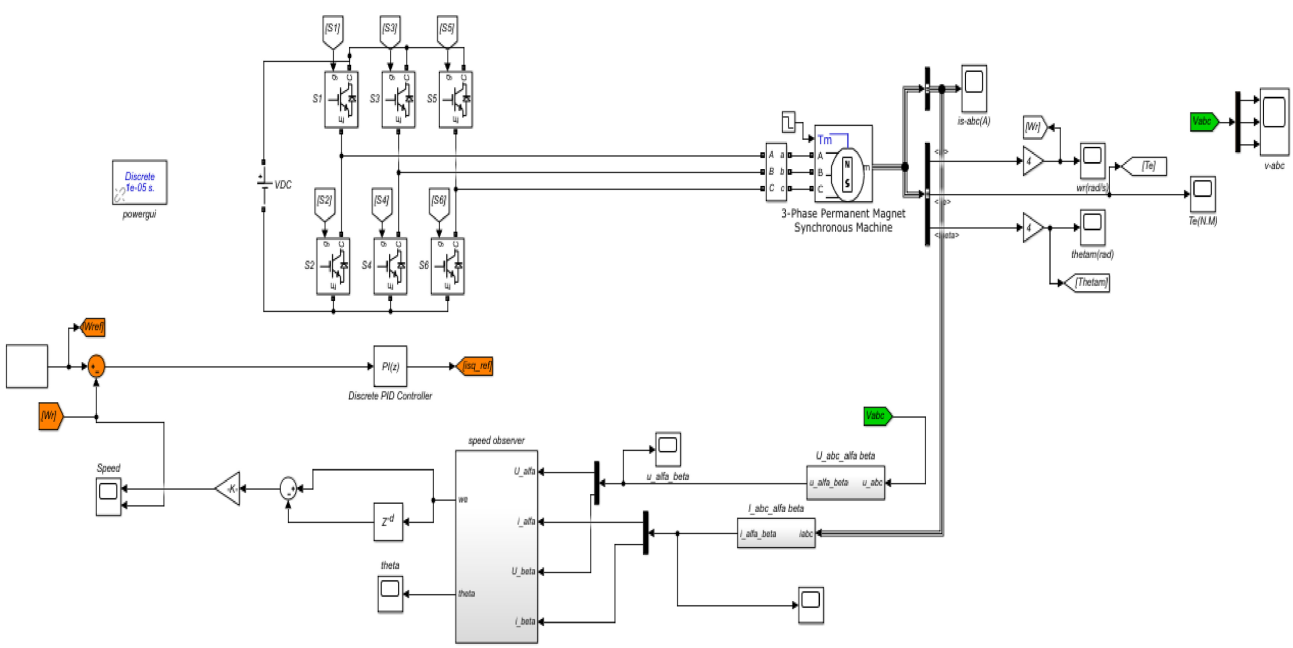

Fig. 17 PMLSM sensor control block diagram

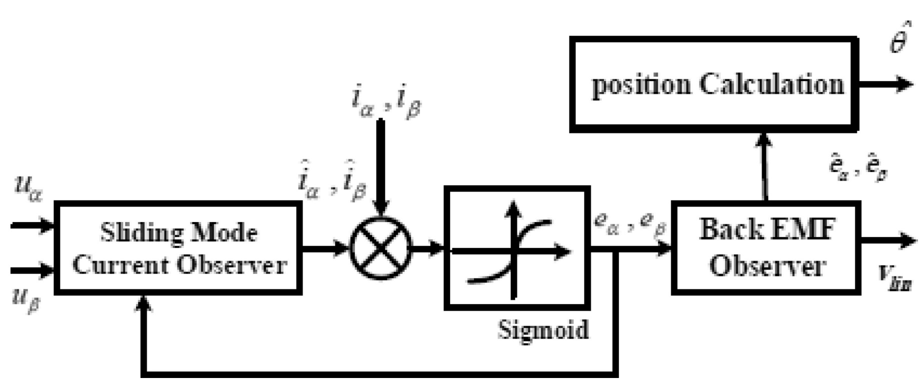

Fig. 18 The proposed sliding mode observer (PSMO) is shown in a block diagram

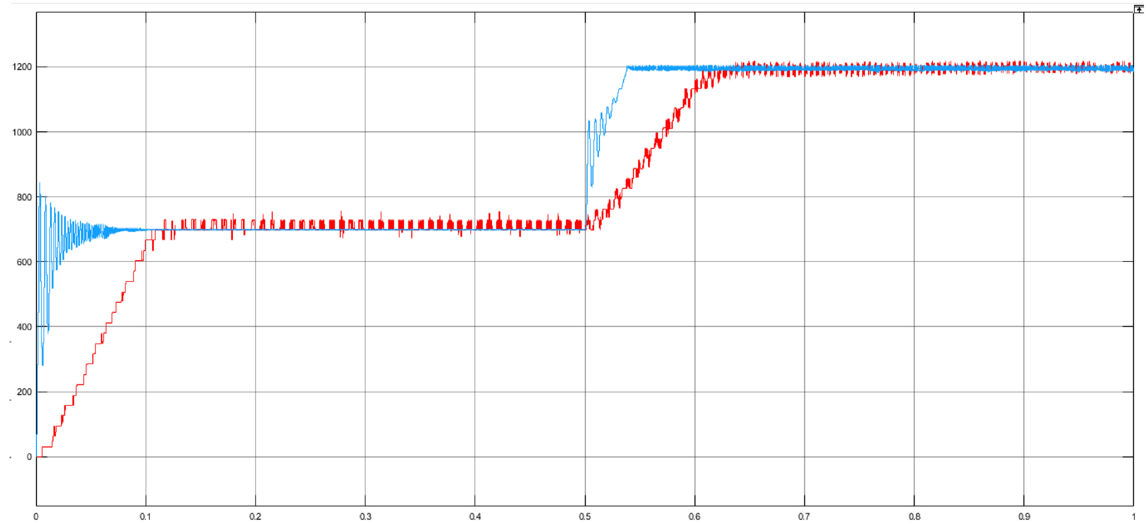

Fig. 19 Both real and estimated speeds

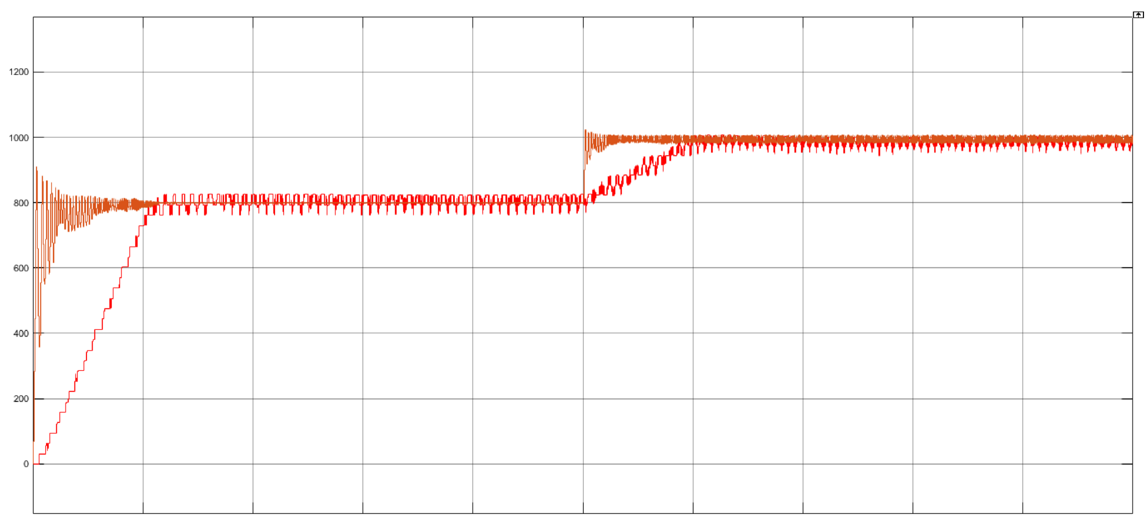

Fig. 20 Real speed and speed estimator

Table 1 Comparing the details of the proposed model with a quantitative method

Control method	Over-shoot (%)	Setting time (s)	Speed during disturbance		Steady state error (rpm)	Rise time (ms)
			Decrease (rpm)	Increase (rpm)		
Speed: PI Current: PI	27	0.4	– 242	338	±19	5.0
Speed: SMC Current: PI	1	1.28	– 247	49	±14	4.4
Speed: FMPC+SMC Current: PI	1	1.08	– 113	19	±14	3.8
Speed: FMPC+SMC Current: FMPC+PI	1	0.546	– 29	19	±11	2.61

Conclusion

In this study, the MPC of a PMSM is studied. The mathematical model of the motor and Simulink modeling of the MPC method are presented. The simulation results show that the designed MPC can improve motor characteristics. Also, the main algorithm is programmed for practical applications. The speed responses show that the MPC performs better than the conventional controllers, as shown in the simulation results. It is shown that MPC can fast track with small constant errors in speed adjustment, and the speed obtained from the fuzzy control methods has a smaller overshoot and shorter settling time under various speed changes. The important point in this study is the use of fuzzy controllers compared to conventional PI controllers. The speed response might be limited to motor changes. The simulation results show the feasibility and efficiency of the MPC method. This control method might be a promising candidate for PMSM control in the future. The key point in this study is the use of a sliding mode estimator for estimating speed with high accuracy, which can be implemented in the speed range of the motor very well. Finally, the following results are obtained.

- Increasing system stability for responding to speed and load changes.
- Reducing the steady-state error towards zero.
- Reducing the torque ripple and current by over 60%.
- Reducing the settling time by 50% and increasing the speed by two–three times using the fuzzy controller compared to the conventional PI controller.
- Using a sliding mode estimator with minimum motor speed deviation.

It is shown that MPC is a fundamental improvement in transient reactions compared to the classic FOC. The predictive deadbeat controller provides a current ripple competitive to FOC. However, it is difficult to improve the steady-state error of FOC. The designed predictive controller, including the dead time, ignores the voltage error resulting from voltage drop in the transistors, diodes and switching time of the transistors because their impact is negligible and their value is variable. To achieve maximum accuracy, the DC voltage error estimation, including a non-linearizing converter, should be considered.

The MPC method can provide minimum transient reaction and reduce the ripple to improve the steady-state response using the modulation proposed in Zhang et al. (2022). It should be mentioned that the modulator also presents a useful correction frequency.

Also, it should be noted that a voltage with a smaller DC connection, higher sampling frequency or higher motor induction improves the MPC current ripple. Each factor facilitates converting the current to a smaller multivariate and more accurate current reference tracking. Therefore, in another experiment with these characteristics, the MPC can be compared. If the MPC is implemented, new constraints, including minimization of switching losses, are added due to its excellent performance that can be studied. Finally, the following items are suggested for future studies:

- Changing the MPC program to improve control of switches' pulses.
- Using a fuzzy PI controller, its coefficients are improved adaptively with the fuzzy controller.
- Using other algorithms for generating switch pulse.

Acknowledgements This work was supported by the project of the Jilin Provincial Department of Education, and the number is JJKH20221301KJ and JJKH20221300KJ.

Author contributions JW: Methodology, software, formal analysis, language review. DYU: Writing—original draft preparation, conceptualization, supervision, project administration.

Data Availability The authors do not have permissions to share data.

Declarations

Conflict of interest The authors declare no competing interests.

References

Ab Ghani, M.S., Zin, N.M., Zakaria, F., Omar, M.F., Yusof, Y., Bohari, A.A.B., Yi, S.S.: Speed control design for permanent magnet synchronous motor drive based on pid-fuzzy controller. In: 2022 3rd International Conference on Artificial Intelligence and Data Sciences (AiDAS), pp. 170–175. IEEE, Washington DC (2022)

Alexandrou, A.D., Adamopoulos, N.K., Kladas, A.G.: Development of a constant switching frequency deadbeat predictive control technique for field-oriented synchronous permanent-magnet motor drive. IEEE Trans. Industr. Electron. **63**(8), 5167–5175 (2016)

Alqudah, A., Mohaidat, M., Altawil, I.: Control of variable speed drive (VSD) based on diode clamped multilevel inverter using direct torque control and fuzzy logic. In: 2013 IEEE Jordan Conference on Applied Electrical Engineering and Computing Technologies (AEECT), pp. 1–6. IEEE, Washington DC (2013)

Cao, C., Wang, J., Kwok, D., Zhang, Z., Cui, F., Zhao, D., Li, M.J., Zou, Q.: webTWAS: a resource for disease candidate susceptibility genes identified by transcriptome-wide association study. Nucleic Acids Res. **50**(1), 1123–1130 (2022)

Cao, Z., Niu, B., Zong, G., Zhao, X., Ahmad, A.M.: Active disturbance rejection-based event-triggered bipartite consensus control for nonaffine nonlinear multiagent systems. Int. J. Robust Nonlinear Control (2023). https://doi.org/10.1002/rnc.6746

Chen, C., Chen, Z., Li, Y., Liu, X., Guo, Y.: A novel self-tuning speed control scheme for the permanent magnet synchronous motor. In: The proceedings of the 17th annual conference of China Electrotechnical Society: vol. II, pp. 649–661. Springer, Singapore (2023)

Du, H., Wen, G., Cheng, Y., Lü, J.: Design and implementation of bounded finite-time control algorithm for speed regulation of permanent magnet synchronous motor. IEEE Trans. Industr. Electron. **68**(3), 2417–2426 (2020)

Duan, J., Wang, S., Sun, L.: Backstepping sliding mode control of a permanent magnet synchronous motor based on a nonlinear disturbance observer. Appl. Sci. **12**(21), 11225 (2022)

Kakosimos, P., Abu-Rub, H.: Predictive speed control with short prediction horizon for permanent magnet synchronous motor drives. IEEE Trans. Power Electron. **33**(3), 2740–2750 (2017)

Kakouche, K., Oubelaid, A., Mezani, S., Rekioua, D., Rekioua, T.: Different control techniques of permanent magnet synchronous motor with fuzzy logic for electric vehicles: analysis, modelling, and comparison. Energies **16**(7), 3116 (2023)

Khezri, E., Zeinali, E.: A review on highway routing protocols in vehicular ad hoc networks. SN Comput. Sci. **2**, 1–22 (2021)

Khezri, E., Zeinali, E., Sargolzaey, H.: A novel highway routing protocol in vehicular ad hoc networks using VMaSC-LTE and DBA-MAC protocols. Wirel. Commun. Mobile Comput. (2022). https://doi.org/10.1155/2022/1680507

Khezri, E., Zeinali, E., Sargolzaey, H.: SGHRP: Secure Greedy Highway Routing Protocol with authentication and increased privacy in vehicular ad hoc networks. PLoS ONE **18**(4), e0282031 (2023)

Li, H., Song, B., Chen, T., Xie, Y., Zhou, X.: Adaptive fuzzy PI controller for permanent magnet synchronous motor drive based on predictive functional control. J. Franklin Inst. **358**(15), 7333–7364 (2021)

Mahmoudi, H., Aleenejad, M., Ahmadi, R.: Modulated model predictive control for a Z-source-based permanent magnet synchronous motor drive system. IEEE Trans. Industr. Electron. **65**(10), 8307–8319 (2017)

Morteza, A., Sadipour, M., Fard, R.S., Taheri, S., Ahmadi, A.: A dagging-based deep learning framework for transmission line flexibility assessment. IET Renew. Power Gener. **17**(5), 1092–1105 (2023)

Ning, Xu., Chen, Z., Niu, B., Zhao, X.: Event-triggered distributed consensus tracking for nonlinear multi-agent systems: a minimal approximation approach. IEEE J. Emerg. Sel. Top. Circuits Syst. (2023). https://doi.org/10.1109/JETCAS.2023.3277544

Raj, F.V.A., Kannan, V.K., Lakshmanan, M., Chitra, K., Srimathi, R., Rubavathy, S.J., Ponmurugan, P.: Performance metric evaluation of a nonlinear fractional order PID controller based on an extended state observer for permanent magnet synchronous motor speed control. In: AIP Conference Proceedings, vol. 2725(1), p. 030006. AIP Publishing LLC, Baltimore (2023)

Sahebjam, M., Sharifian, M.B., Feyzi, M.R., Sabahi, M.: Novel methodology for direct speed control of a permanent magnet synchronous motor with sensorless operation. IET Electr. Power Appl. **15**(6), 728–741 (2021)

Samiei, M., Hassani, A., Sarspy, S., Komari, I.E., Trik, M., Hassanpour, F.: Classification of skin cancer stages using a AHP fuzzy technique within the context of big data healthcare. J. Cancer Res. Clin. Oncol. **149**(11), 8743–8757 (2023)

Saraei, N., Khanal, M., Tizghadam, M.: Removing acidic yellow dye from wastewater using *Moringa peregrina*. Comput. Res. Prog. Appl. Sci. Eng. **8**, 1–8 (2022). https://doi.org/10.52547/crpase.8.3.2483

Sun, J., Zhang, Y., Trik, M.: PBPHS: a profile-based predictive handover strategy for 5G networks. Cybern. Syst. **53**(6), 1–22 (2022)

Trik, M., Mozaffari, S.P., Bidgoli, A.M.: Providing an adaptive routing along with a hybrid selection strategy to increase efficiency in NoC-based neuromorphic systems. Comput. Intell. Neurosci. (2021). https://doi.org/10.1155/2021/8338903

Trik, M., Molk, A.M.N.G., Ghasemi, F., Pouryeganeh, P.: A hybrid selection strategy based on traffic analysis for improving performance in networks on chip. J. Sensors (2022). https://doi.org/10.1155/2022/3112170

Trik, M., Akhavan, H., Bidgoli, A.M., Molk, A.M.N.G., Vashani, H., Mozaffari, S.P.: A new adaptive selection strategy for reducing latency in networks on chip. Integration **89**, 9–24 (2023)

Ullah, K., Guzinski, J., Mirza, A.F.: Critical review on robust speed control techniques for permanent magnet synchronous motor (PMSM) speed regulation. Energies **15**(3), 1235 (2022)

Vijay Amrith Raj, V., Kamatch Kannan, V.: Adaptive ELM neural computing framework with fuzzy PI controller for speed regulation in permanent magnet synchronous motors. Soft. Comput. **24**, 10963–10980 (2020)

Xu, W., Jiang, Y., Mu, C.: Novel composite sliding mode control for PMSM drive system based on disturbance observer. IEEE Trans. Appl. Supercond. **26**(7), 1–5 (2016)

Ye, S., Yao, X.: A modified flux sliding-mode observer for the sensorless control of PMSMs with online stator resistance and inductance estimation. IEEE Trans. Power Electron. **35**(8), 8652–8662 (2020)

Zhang, H., Zou, Q., Ju, Y., Song, C., Chen, D.: Distance-based support vector machine to predict DNA N6-methyladine modification. Curr. Bioinform. **17**(5), 473–482 (2022)

Zhang, H., Zhao, X., Wang, H., Niu, B., Xu, N.: Adaptive tracking control for output-constrained switched MIMO pure-feedback nonlinear systems with input saturation. J. Syst. Sci. Complex. **36**, 960–984 (2023)

Zhao, H., Wang, H., Niu, B., Zhao, X., Alharbi, K.H.: Event-triggered fault-tolerant control for input-constrained nonlinear systems with mismatched disturbances via adaptive dynamic programming. Neural Netw. **164**, 508–520 (2023)